A Multi-Optional Adjustable IHS-BT Approach for High Resolution Optical and SAR Image Fusion

Yu Su[1*], Ching-Hai Lee[2], and Te-Ming Tu[3]

[1]*Department of Computer Science and Information Engineering, Yuanpei University*
[2]*Department of Information Communication, Mingdao University*
[3]*Department of Digital Content and Technology, Ta Hwa University of Science and Technology*

ABSTRACT

It is well known that the photo-interpretation of radar images is substantially different from the optical images due to *SAR*'s scattering mechanism. Merging optical images with *SAR* imagery can provide complementary information in order to improve understanding the structure of the features within the *SAR*. To achieve the goal, this research has developed an extension model of the *IHS-BT* approach (*eIHS-BT*) with multi-optional adjustments for image fusion. The model provides four fusion methods of *Pan-MS, SAR-MS, SAR-Pan-MS* and *SAR-Pan* by setting two parameters. Apart from that, the *SAR-Pan-MS* or *SAR-Pan* image fusion method can show better performance in assisting *SAR* image understanding because of reasonable contents of spatial details and texture features by tuning one parameter for adjusting the proportion of *Pan* to *SAR* image information. In the mean time, an effectively red-green viewer (RGV) to increase the quality of the radar images is introduced to assist object recognition by reducing the bright star effect.

Keywords: Intensity-Hue-Saturation fusion, Brovey transform, Synthetic Aperture Radar.

多重調整 IHS-BT 高解析光學及雷達影像融合法

蘇有[1*]　李靖海[2]　杜德銘[3]

[1]元培科技大學資訊工程系
[2]明道大學資訊傳播學系
[3]大華科技大學數位內容科技系

摘　　要

由於雷達電磁波的散射與反射機制，造成了 *SAR* 雷達影像與光學影像的影像解譯方式有非常大的差異。因此，在 *SAR* 雷達影像中整合光學影像以補充地表相關資訊，即可強化我們對於 *SAR* 雷達影像特徵結構的瞭解。為了完成以上之目標，本文除了詳述了雷達影像與光學影像的特性之外，還提出了一個具有多種選擇調整機制的影像融合方法--「擴充光譜調整的 *IHS-BT* 方法」，此方法利用二個可調參數的設定而提供了四種影像融合方式。此外，從本研究之實驗成果看出，善加調整「衛星光學全色態影像、多光譜影像與 *SAR* 雷達影像融合」方法中光學全色態影像與 *SAR* 雷達影像的資訊融合比例，可以有效的輔助本研究對 *SAR* 雷達影像中空間細節及紋理特徵的理解。

關鍵詞：IHS融合、BT轉換、合成孔徑雷達

文稿收件日期 101.6.14; 文稿修正後接受日期 102.4.16 ; *通訊作者
Manuscript received June 14, 2012; revised April 16, 2013; * Corresponding author

Ⅰ. INTRODUCTION

Nowadays, both optical satellites(such as IKONOS, QuickBird, GeoEye-1, WorldView) and *SAR* satellites (TerraSAR-X, Cosmo Sky Med, RadarSat-2) can provide very high resolution image data. These two types of imagery have their own characteristics. *SAR*, an active sensor, can collect ground surface data during day and night without being affected by weather conditions, and sense the structure of terrain features such as topography, thickness and roughness of surface. Besides, features of the geometric structure of manmade objects become observable. On the other hand, optical sensors sense the electromagnetic energy reflected from the ground surface. Due to the fact that many land cover materials have similar spectra, it is extremely hard to analyze a scene when only an optical sensor is used. On the contrary, discriminations of some features can be shown in *SAR* images because of their dielectric properties and geometric structure. The discriminations assist image analysts to interpret the features. Therefore, interpretation of the features in *SAR* data is a field of rapidly growing importance in remote sensing. But, *SAR* image interpretation without context information is often difficult even for experts due to the special viewing geometry and the presence of the *SAR* phenomena of foreshortening, layover, shadow, total reflection, and multi-bounce scattering. In order to overcome the shortcomings, *SAR* images are fused with optical images. Therefore, the image interpretation can benefit from an integration of detailed spatial and color information in the analysis of *SAR* images. With the aid of complementary information the analyst can study a given image of the features and discriminate relatively small details. *SAR* image interpretation becomes not difficult to carry out and in the mean time the image interpreters learn ability to discern the exact details of the features by the obtained interpretation results. Hence new *SAR* image interpreters can train themselves to familiar with the *SAR* phenomena by interpreting *SAR* imagery fused with Optical images.

It is widely accepted that image fusion is capable of creating more information by means of merging different imagery. Generally, most of standard image fusion techniques are used for fusing high resolution panchromatic (*Pan*) images with low resolution multispectral (*MS*) images. These techniques are such as intensity-hue-saturation transform (IHS), Brovery transform (BT), principal component transform (PCA), additive wavelet transform (AWT), smoothing filter-based intensity modulation (SFIM) and other new approaches [1-8]. As these techniques applied to fusing *SAR* images, a Pan image is usually replaced by *SAR* imagery. As a result of that, *SAR* image interpretation is carried out with color information from *MS* imagery but without detailed spatial information from the *Pan* image. Surely better interpretation results can be given by fusing *SAR* image with both color and detailed spatial information. To meet this demand, the fusion method has to be able to fuse *SAR*, *Pan* and *MS* imagery. This work presents a new technique for *SAR*-Optical image fusion, which allows not only

(1) fusing high resolution *Pan* images with low resolution *MS* images and
(2) fusing high resolution *SAR* images with low resolution *MS* images, but also
(3) fusing high resolution *Pan* images with *SAR* images and
(4) fusing *SAR* and *Pan* images with *MS* images at a desired degree of information from *SAR* and *Pan* images.

The proposed technique, an extension model of *IHS-BT* approach (*eIHS-BT*), has two adjustable parameters. One is to choose the approach as an *IHS*, *BT* or *IHS-BT* image fusion function, and the other is to alter the proportion of *Pan* to *SAR* image information in the process of fusing *SAR* and *Pan* images with *MS* images.

Due to the cover effect of strong bright stars caused by corner reflections, the original 11 bit *SAR* image is usually hard to interpret. For the purpose of reducing the cover effect and improve the quality of the radar image recognition, a simple red-green viewer is also presented. In order to verify the efficacy of the proposed approach, experiments were carried out on fusing IKONOS and TerraSAR-X images.

Ⅱ. INTEGRATING IHS WITH BT IMAGE FUSION

Among the current high resolution image fusion methods, *IHS* and *BT* techniques can provide satisfying results except the disadvantage of color distortion. The characteristics of the *IHS*, *BT* and *IHS-BT* methods are briefly reviewed as below.

The *IHS* and *BT* methods [9] can be operated respectively by

$$\begin{bmatrix} R'_{IHS} \\ G'_{IHS} \\ B'_{IHS} \end{bmatrix} = \begin{bmatrix} R+(Pan-I) \\ G+(Pan-I) \\ B+(Pan-I) \end{bmatrix} = \begin{bmatrix} R+\delta_{IHS} \\ G+\delta_{IHS} \\ B+\delta_{IHS} \end{bmatrix} \quad \text{and}$$

$$\begin{bmatrix} R'_{BT} \\ G'_{BT} \\ B'_{BT} \end{bmatrix} = \frac{Pan}{I} \cdot \begin{bmatrix} R \\ G \\ B \end{bmatrix} = \gamma_{BT} \cdot \begin{bmatrix} R \\ G \\ B \end{bmatrix} \tag{1}$$

where $\delta_{IHS} = Pan - I, \quad I = (R + G + B)/3,$ and $\gamma_{BT} = Pan / I.$ From the viewpoint of signal analysis, γ_{BT} is a modulation factor to modulate signals while δ_{IHS} is an injection factor to increase signal strength for image fusion. Both of them can be treated as the spatial details from the fused *Pan* image. If the *Pan* image replace by a high resolution *SAR* image (TerraSAR, Cosmo Sky Med, and Radarsat-II) in (1), both *IHS* and *BT* also can fuse *SAR* data with low resolution *MS* images. That is

$$\begin{bmatrix} R'_{IHS} \\ G'_{IHS} \\ B'_{IHS} \end{bmatrix} = \begin{bmatrix} R+(SAR-I) \\ G+(SAR-I) \\ B+(SAR-I) \end{bmatrix} = \begin{bmatrix} R+\delta'_{IHS} \\ G+\delta'_{IHS} \\ B+\delta'_{IHS} \end{bmatrix} \quad \text{and}$$

$$\begin{bmatrix} R'_{BT} \\ G'_{BT} \\ B'_{BT} \end{bmatrix} = \frac{SAR}{I} \cdot \begin{bmatrix} R \\ G \\ B \end{bmatrix} = \gamma'_{BT} \cdot \begin{bmatrix} R \\ G \\ B \end{bmatrix} \tag{2}$$

Where $\delta'_{IHS} = SAR - I,$ and $\gamma'_{BT} = SAR / I.$

To evaluate these two image fusion methods, two *RGB-IHS* conversion models are used. The first one is a linear transformation [10]:

$$\begin{bmatrix} I \\ v1 \\ v2 \end{bmatrix} = \begin{bmatrix} 1/3 & 1/3 & 1/3 \\ -\sqrt{2}/6 & -\sqrt{2}/6 & 2\sqrt{2}/6 \\ 1/\sqrt{2} & -1/\sqrt{2} & 0 \end{bmatrix} = \begin{bmatrix} R \\ G \\ B \end{bmatrix} \quad \text{and}$$

$$\begin{bmatrix} R \\ G \\ B \end{bmatrix} = \begin{bmatrix} 1 & -1/\sqrt{2} & 1/\sqrt{2} \\ 1 & -1/\sqrt{2} & -1/\sqrt{2} \\ 1 & \sqrt{2} & 0 \end{bmatrix} \begin{bmatrix} I \\ v1 \\ v2 \end{bmatrix} \tag{3}$$

Hue (*H*) and saturation (*S*) are defined by the internal variables *v*1 and *v*2, and represented as

$$H = \tan^{-1}\left(\frac{v2}{v1}\right) \quad \text{and}$$

$$S = \sqrt{v1^2 + v2^2} \tag{4}$$

An alternative *RGB-IHS* conversion model is a nonlinear transformation. That is defined by

$$I = [R + G + B]/3 \tag{5-1}$$

$$H = \begin{cases} \cos^{-1}(\varphi), & \text{if } G \geq R \\ 2\pi - \cos^{-1}(\varphi), & \text{if } G \leq R \end{cases} \quad \text{and}$$

$$\varphi = \frac{(2B - G - R)/2}{\sqrt{(B-G)^2 + (B-R)(G-R)}} \tag{5-2}$$

$$S = 1 - \frac{3\min(R,\ G,\ B)}{R+G+B} = \frac{I-a}{I} \quad \text{and}$$

$$a = \min(R,\ G,\ B) \tag{5-3}$$

According to theoretically expectations and experimental results [9], both *IHS* and *BT* can maintain the spatial details from the *Pan* (or *SAR*) image, but distort the saturation component rather than the hue information. The *IHS* method works properly under the nonlinear *RGB-IHS* conversion system, while the *BT* method works in the linear *RGB-IHS* conversion system. For the most of vegetation zones, the *IHS* suffers from color distortion on saturation compression, while *BT* distorted on saturation stretching. This is the main difference between *IHS* and *BT* in color distortion problems.

The following saturation component ratios of fused images by *IHS* and *BT* technique respectively are important to equations listed behind:

$$S'_{IHS} = 1 - \frac{3\min(R+\delta_{IHS},\ G+\delta_{IHS},\ B+\delta_{IHS})}{R+G+B+3\delta_{IHS}}$$

$$= \frac{I-a}{Pan} = \frac{I}{Pan} \cdot S \tag{6-1}$$

$$S'_{BT} = \sqrt{(\gamma_{BT} \cdot v1)^2 + (\gamma_{BT} \cdot v2)^2}$$

$$= \gamma_{BT} \cdot \sqrt{v1^2 + v2^2} = \frac{Pan}{I} \cdot S \tag{6-2}$$

$$\frac{S'_{IHS}}{S} = \frac{I}{Pan} \quad \text{and} \quad \frac{S'_{BT}}{S} = \frac{Pan}{I} \tag{6-3}$$

To reduce the color distortion, according to equation (6), an adjustable *IHS-BT* approach [10] is designed for balancing saturation by adjusting a parameter to control the degree of saturation stretch/compression in the fused image. The method is modeled as

$$\begin{bmatrix} R'_{IHS\text{-}BT} \\ G'_{IHS\text{-}BT} \\ B'_{IHS\text{-}BT} \end{bmatrix} = \frac{Pan}{I + k \cdot (Pan - I)} \begin{bmatrix} R + k \cdot (Pan - I) \\ G + k \cdot (Pan - I) \\ B + k \cdot (Pan - I) \end{bmatrix} = \frac{Pan}{I + k \cdot (Pan - I)} \begin{bmatrix} R' \\ G' \\ B' \end{bmatrix} \tag{7}$$

Where k is a weighting parameter used to control the degree of saturation stretch / compression, and its suggested value is between 0 and 1 (i.e., $0 \le k \le 1$). The intensity and hue components are the same as the original *Pan* and *MS* image, respectively. That is

$$I'_{IHS\text{-}BT} = \left[R'_{IHS\text{-}BT} + G'_{IHS\text{-}BT} + B'_{IHS\text{-}BT} \right] / 3 = Pan \tag{8}$$

$$H'_{IHS\text{-}BT} = H' = H \tag{9}$$

However, the saturation component ratio, based on equation (7), is derived as following:

$$\begin{bmatrix} R' \\ G' \\ B' \end{bmatrix} = \begin{bmatrix} R + k \cdot (Pan - I) \\ G + k \cdot (Pan - I) \\ B + k \cdot (Pan - I) \end{bmatrix} \tag{10}$$

$$I' = \left[R' + G' + B' \right] / 3 = I + k \cdot (Pan - I) \tag{11}$$

$$S' = \frac{I}{I + k \cdot (Pan - I)} \cdot S \tag{12}$$

$$\frac{S'_{IHS\text{-}BT}}{S} = \frac{S'_{IHS\text{-}BT}}{S'} \cdot \frac{S'}{S} = \frac{I'_{IHS\text{-}BT}}{I'} \cdot \frac{I}{I'} = \frac{Pan}{I + k \cdot (Pan - I)} \cdot \frac{I}{I + k \cdot (Pan - I)} \tag{13}$$

As k‘s value is 0, the saturation component ratio is identical to the *BT* method. So in this case, *IHS-BT* method is identical with the *BT* method. It becomes the *IHS* method as $k = 1$. And when k‘s value is greater than 0 but less than 1, the saturation component ratio is adjusted to lie in between those of *IHS* and *BT*. For the purpose of saturation balance, $k = 0.5$ might be a good and reasonable choice.

Decreasing the value of $\delta_{IHS}\,(i.e., Pan - I)$ by adjusting appropriately spectra is also a method to reduce the color distortion of *IHS-BT* fusion imagery. Considering the spectral mismatch between the *Pan* and *MS* imagery, the grey value difference between the *I* band and *Pan* imagery can be efficiently reduced by means of introducing the near infrared (*NIR*) band into the *I* band [13]. So that, the functional relationship of the gray values between *Pan* imagery and each band of *MS* (*R*, *G*, *B* and *NIR*) can be stated as equation (14) including four weight factors of *a*, *b*, *c* and d [11, 12]. As the four weight factors are given proper values for IKONOS, QuickBird, and GeoEye imagery, the *IHS-BT* method can work well for fusing high resolution *Pan* data with low resolution *MS* images [12].

$$Pan \approx a \cdot R + b \cdot G + c \cdot B + d \cdot NIR = I \tag{14}$$

It is suggested that *Pan* imagery be replaced with high resolution *SAR* imagery when the *IHS-BT* method is applied to fusing *SAR* data with low resolution *MS* images. Then, equations (7) and (13) can be rearranged respectively as (15) and (16).

$$\begin{bmatrix} R'_{IHS\text{-}BT} \\ G'_{IHS\text{-}BT} \\ B'_{IHS\text{-}BT} \end{bmatrix} = \frac{SAR}{I + k \cdot (SAR - I)} \begin{bmatrix} R + k \cdot (SAR - I) \\ G + k \cdot (SAR - I) \\ B + k \cdot (SAR - I) \end{bmatrix} = \frac{SAR}{I + k \cdot (SAR - I)} \begin{bmatrix} R' \\ G' \\ B' \end{bmatrix} \tag{15}$$

$$\frac{S'_{IHS\text{-}BT}}{S} = \frac{S'_{IHS\text{-}BT}}{S'} \cdot \frac{S'}{S} = \frac{I'_{IHS\text{-}BT}}{I'} \cdot \frac{I}{I'} = \frac{SAR}{I + k \cdot (SAR - I)} \cdot \frac{I}{I + k \cdot (SAR - I)} \tag{16}$$

Adjusting spectra to reduce the color distortion is no longer available for *SAR-MS* fusion owing to the different characters existing between *SAR* and optical data. Therefore, the spectral distortion caused by fully injecting *SAR* features into multispectral imagery is not avoidable.

Ⅲ. THE IHS-BT EXTENSION AND RED-GREEN VIEWER

Due to an increasing in the number of high resolution *SAR* and optical images, a flexible *SAR*-Optical fusion technique becomes much more important to interpretation and information extraction from fused images with corresponding features showing at the same time and pixel. High resolution *Pan* imagery allow for a more accurate understanding of phenomena on the ground in which individual trees, automobiles, road networks, and houses are clearly visible. For preserving the original *SAR* and *Pan* information, it is desired to have an option to adjust the proportion between *SAR* and *Pan* imagery in the fusion processing. For doing so, we can't just fuse *SAR* imagery with *MS* imagery based on equation (2) or (15). To tackle this problem, an extension model of *IHS-BT* approach (*eIHS-BT*) with multi-optional adjustments is designed as follows:

$$\begin{bmatrix} R'_{eIHS\text{-}BT} \\ G'_{eIHS\text{-}BT} \\ B'_{eIHS\text{-}BT} \end{bmatrix} = \frac{Pan}{I + k \cdot (Pan - I)} \begin{bmatrix} R + k \cdot (Pan - I) \\ G + k \cdot (Pan - I) \\ B + k \cdot (Pan - I) \end{bmatrix} + (1 - l) \begin{bmatrix} SAR - Pan \\ SAR - Pan \\ SAR - Pan \end{bmatrix} \quad (17)$$

where *k*'s function is the same as that of *k* in equation (7), *l* ranged from 0 to 1 ($0 \le l \le 1$) is a parameter to adjust the proportions of *SAR* and *Pan* information fused with *MS* imagery. Besides, either *SAR* or *Pan* information is chosen when *l* is valued as 0 or 1, whereas parts of two information are chosen when $0 < l < 1$. The intensity component and saturation component ratio of a fused image by the *eIHS-BT* method are rewritten as (18) and (19) respectively.

$$I'_{eIHS\text{-}BT} = \left[R'_{eIHS\text{-}BT} + G'_{eIHS\text{-}BT} + B'_{eIHS\text{-}BT} \right] / 3 = Pan; \quad when\ l = 1\ and\ 0 \le k \le 1 \quad (18\text{-}1)$$

$$I'_{eIHS\text{-}BT} = \left[R'_{eIHS\text{-}BT} + G'_{eIHS\text{-}BT} + B'_{eIHS\text{-}BT} \right] / 3 = SAR; \quad when\ l = 0\ and\ 0 \le k \le 1 \quad (18\text{-}2)$$

$$I'_{eIHS\text{-}BT} = \left[R'_{eIHS\text{-}BT} + G'_{eIHS\text{-}BT} + B'_{eIHS\text{-}BT} \right] / 3 = Pan + (1 - l)(SAR - Pan) = l \cdot Pan + (1 - l) \cdot SAR; \quad when\ 0 < l < 1\ and\ 0 \le k \le 1 \quad (18\text{-}3)$$

$$\frac{S'_{eIHS\text{-}BT}}{S} = \frac{P}{I + k \cdot (P - I)} \cdot \frac{I}{I + k \cdot (P - I)}, \quad where\ P = l \cdot Pan + (1 - l) \cdot SAR \quad (19)$$

Equation (18-3) offers a fusion method (*SAR-Pan*) for fusing *SAR* and *Pan* images as an image $I'_{eIHS\text{-}BT}$ of which information from *SAR* and *Pan* can be adjusted with l. Table 1 summarizes the fusion methods and images of the *eIHS-BT* approach. As compared with the standard fusion methods, the proposed method shows one advantage of being able to control the amount of spatial detail, spectral content and texture structure in the fused image by changing the values of *k* and *l* used in fusion process.

Table 1. Fusion methods and images chosen by two parameters of the *eIHS-BT* approach

Parameters		Fused images			Image fusion methods			
l	*k*	*MS*	*Pan*	*SAR*	*IHS*	*BT*	*IHS-BT*	*SAR-Pan*
1	1	✓	✓		✓			
	0					✓		
	0<*k*<1						✓	
0	1	✓		✓	✓			
	0					✓		
	0<*k*<1						✓	
0<*l*<1	1	✓	✓	✓	✓			
	0					✓		
	0<*k*<1						✓	
	0<*k*<1		✓	✓				✓

Since grey levels in a *SAR* image related to the microwave backscattering properties of the surface, the intensity of the backscattered signal varies according to the material and the construction. Hence the *SAR* image refers mainly to geometrical properties of the objects. The objects such as buildings and vehicles are always have strong corner reflections appear as bright stars in the image that may cover the signal of neighboring objects over wide areas. So the original 11 bit *SAR* image is usually hard to interpret. The phenomenon burdens the interpretation of the *SAR* imagery even for experts. To ease this issue, this work develops a Red-Green Viewer (RGV) for lightening the impact of the bright stars and retaining main source points of them. For achieving this goal, the RGV is developed by following steps:

(1) For reducing bright stars, cutting off minimum/maximum 0.5% to 1% of gray levels is applied to adjusting the dynamic

range of *SAR* image, followed by a linear stretching to scale the 11-bit image down to an 8-bit image. The 8-bit image is then assigned as *R* image.

(2) Copy the *R* image, convert it to an inverse version, and assign this inversed image as *G* image.

(3) A pseudo color image *T* can be composed by

$$T = \begin{bmatrix} R \\ G \\ 0 \end{bmatrix} \tag{20}$$

In order to verify the performance of the proposed techniques in (17) and (20), real IKONOS and TerraSAR-X images are used in the experiments whose results are shown in the following section.

Ⅳ. EXPERIMENTAL RESULTS AND ANALYSIS

To effectively using the proposed method of *eIHS-BT*, equation (17) has been implemented into a Windows-based program, which consists of two windows, the Scroll window and Main image window. The input image is displayed in the scroll window at a sub-sampled resolution, as shown in the above left side of Fig.1(a). The indicator of the main image window appears as a red box within the scroll window and outlines the area that is displayed in full resolution in the main image window, as shown in the right side of Fig.1(a). The program only reads and fuses the associated images within the main image window in the first phase so as to decrease the time-consuming for adjusting parameters *k* and *l*. As suitable parameters are determined, the fusion is then performed on the entire image. To satisfy various demands, the fusion image displayed in the main or scroll window can be individually selected and stored. Especially by the main window, interested moving or stationary targets can be selected and stored into a knowledge base to train and aid *SAR* image interpreters.

As an illustrated example, the data set used in this approach is extracted from IKONOS *Pan* band (1m), *MS* bands (4m), and TerraSAR-X image (1m) over the Lushun harbor in China, which was acquired on November 15, 2005, and October 2, 2007, respectively. Image fusion essentially occurs when the involved images have the same spatial resolution. Thus, *MS* images need to be resampled such that they have the same spatial resolution as the *Pan* or *SAR* image. For resampling, the cubic interpolation is used. The TerraSAR-X data has been co-registered to the IKONOS *Pan* image, which is geocoded with 8000 *8000 pixels by choosing 25 control points manually.

For the purpose of clear visualization, we only display small chips in all results. The *Pan* image and the corresponding resized *RGB* images of the test data are displayed in Fig.1(a) and Fig.1(b), respectively, while the *SAR* image is shown in Fig.1 (c). To verify the performance of the proposed fusion method, the three images were fused by the same equation (17) but used different values of *k* and *l* individually. The red-green viewer (RGV) was applied on the *SAR* image to verify its performance as well.

Fig.1(d), Fig.1(e) and Fig.1(f) show the results of the *Pan-MS* fusion method by setting *l* = 1 but they were fused in *IHS*, *BT*, or *IHS-BT* method by setting *k* as 1, 0 or 0.5 respectively. It can be easily observed that, the fused images generated by the three fusion methods well demonstrate that all colors are almost unchanged. In terms of spatial details, all spatial features of the *Pan* image are also perfectly injected into the fused images. By visually inspecting spatial features, we can find that *IHS* (Fig.1(d)) has preserved more spatial details than *BT* (Fig.1(e)). The result, shown in Fig.1(f) given by *IHS-BT* method, is similar to that from *IHS* (Fig.1(d)) and can give better performance in preserving both spectral and spatial information. These results demonstrate that the proposed model of *eIHS-BT* has a function of fusing high resolution *Pan* images with low resolution *MS* images in *IHS*, *BT*, or *IHS-BT* method determined by *k* when *l* is set as 1.

The SAR images only provide 1 m resolution for HH and VV modes with $25^{\circ} \sim 55^{\circ}$ incident angle when the flight direction has right/left descending/ascending modes. For a specified target, which mode can generate the best corner scatter characteristics? Equation (17) gives an approach to fuse optical and *SAR* images. *MS* and *Pan* offer the color and target detail information, respectively, while *SAR* provides the texture feature. After many observations for the same area, therefore, we can

find the best mode to build database for the specified target. To present the results of *SAR*-Optical image fusion given by (17), Figure 2 contains the fusion results of the same image by setting different l value. As seen from Fig.2(a), that is a *SAR-MS* image fusion (here k = 0.5 and l = 0) only the texture structures of the *SAR* image are injected into the *MS* image without any spatial detail from the *Pan* image. This leads to an increasing difficulty in interpreting the image.

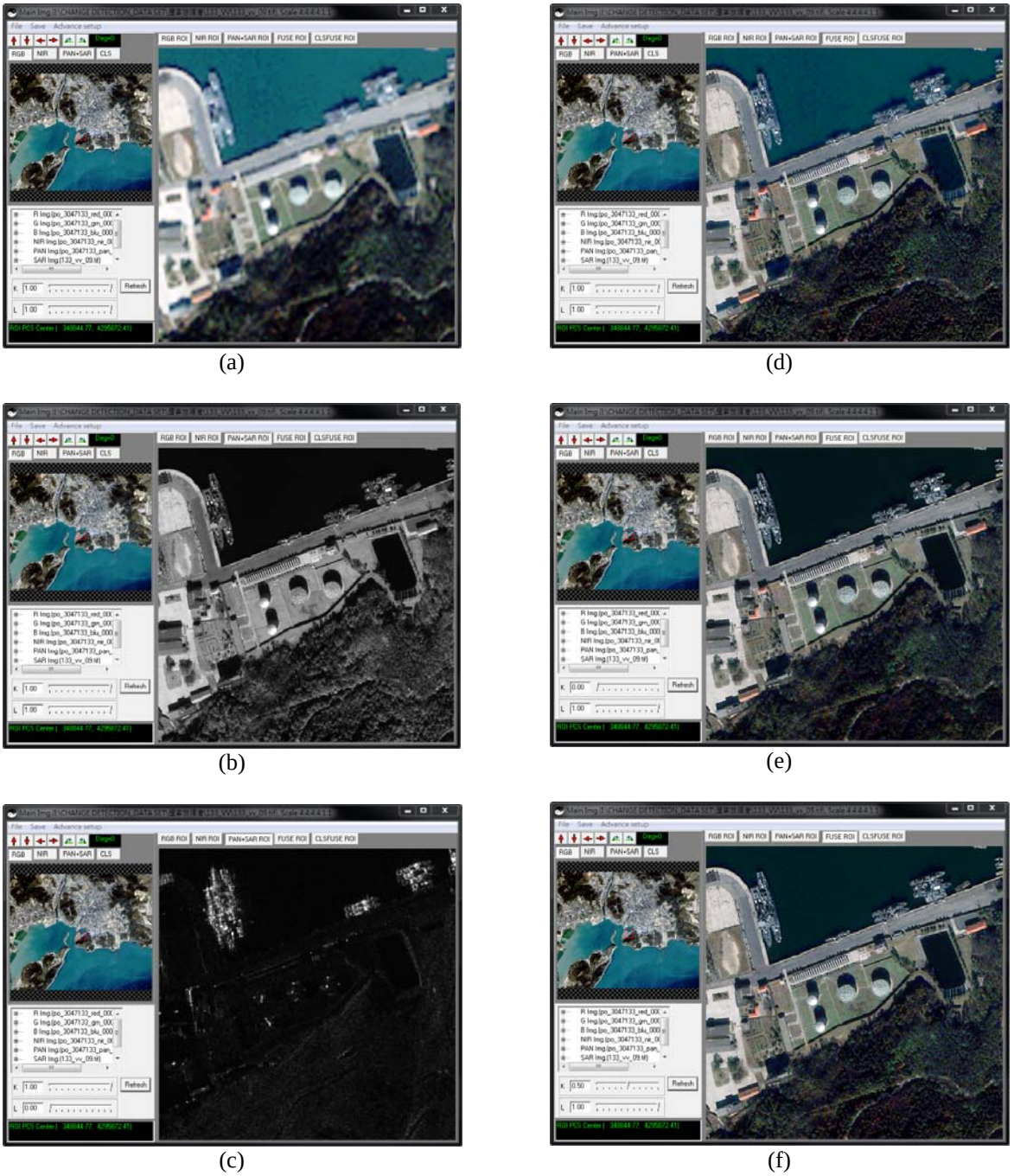

(a) (d)

(b) (e)

(c) (f)

Fig.1. (a) Original IKONOS *RGB* image, (b) Corresponding IKONOS *Pan* image, (c) The TerraSAR-X image, (d) Fused image generated by *IHS*, k = 1 and l = 1, (e) Fused image generated by *BT*, k = 0 and l = 1, (f) Fused image generated by *IHS-BT*, k = 0.5 and l = 1.

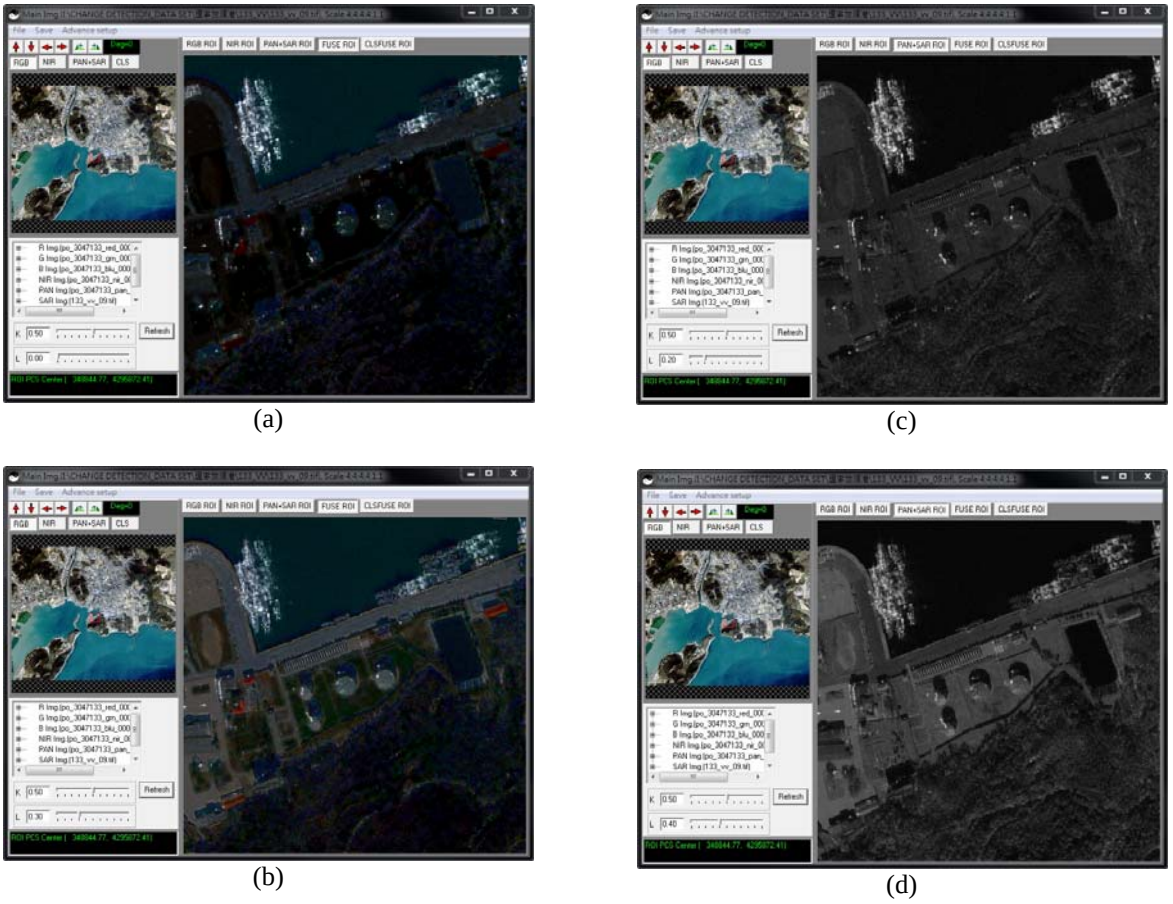

(a) (c)

(b) (d)

Fig.2. (a) Fused image generated by *IHS-BT*, k = 0.5 and l = 0 (this is a *SAR-MS* fusion), (b) Fused image generated by *IHS-BT*, k = 0.5 and l = 0.3 (this is a *SAR-Pan-MS* fusion), (c) This is *SAR-Pan* fusion, 0.8**SAR*+0.2**Pan*, (d) This also is *SAR-Pan* fusion, 0.6**SAR*+0.4**Pan*.

However, the fusion result of *SAR-Pan-MS* (here k = 0.5 and 0 < l < 1) is demonstrated in Fig.2(b) which shows that not only texture structures but also spatial details have been injected into the *MS* image. The spectral information shown in Fig.2(b) is much more than Fig.2(a) but spectral information in both is distorted. With the aids of spectral and spatial information in the fused image, image interpreters can see the surrounding features of texture structures so that image interpretation become easier. According to experiments, increasing l value leads to more spatial details transferred from *Pan* image but less texture structure kept from original *SAR* image. This means that the correlation coefficients among original *SAR* and fused images are decreased. On the contrary, a decrease in value of l will increase the texture structures but decrease the color and spatial details of fused images. Therefore, the flexibility to adjust the proportions of *SAR* and *Pan* information fused with *MS* imagery has been demonstrated. Besides, its performance is better than that given by the way of just fusing *SAR* imagery with *MS* imagery. In our experiments, reasonable results can be given when a recommend value of l = 0.3 is used.

If we average the *RGB* components of the fused image by Eq. (18-3), the results of $I'_{eIHS\text{-}BT}$ can be regarded as a *SAR-Pan* fusion method which fuses *SAR* imagery with *Pan* imagery. Fig.2(c) and Fig.2(d) display the fusion images when l value is 0.2 or 0.4, respectively. That Fig.2(d) shows more spatial details than Fig.2(c) shows an increase in l value increases the information of spatial details from *Pan* imagery. The increased spatial details will assist image interpreters in understanding targets because of the surrounding features of strong corner reflections.

Although the red-green viewer (RGV) is a

simple approach for colorizing an 11 bit *SAR* image, it without any filter or lookup table design, the texture effort is very perfect as display. As seen from Fig.3, the cover effect area of bright stars shown in read color had been reduced but the number of main points of them did not change. As a summary, the RGV can significantly reduce the cover effect visually and preserve the structural information of the original *SAR* images. To effectively using the RGV, it usually geo-link to the other image, such as the original *Pan* or the fused image by the *Pan-MS/SAR-Pan-MS* methods (the geo-link function also has implemented in our program).

In this research we only focus on the visual effect and fusion performance: to keep more detail information from *Pan* and *SAR* image while we need color information from *MS* images.

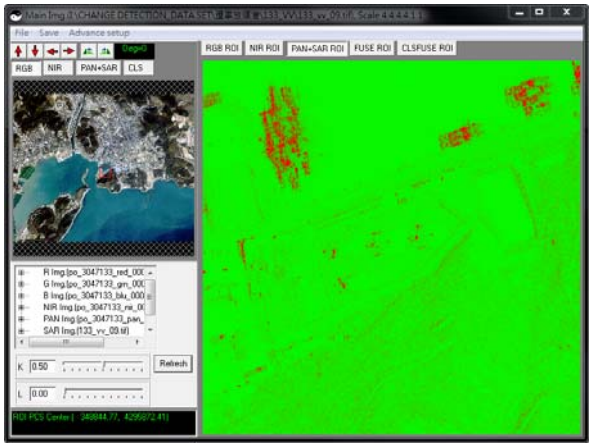

Fig.3. The red-green viewer.

V. CONCLUSIONS

The current image fusion techniques were developed to fuse optical high spatial resolution panchromatic and low spatial resolution multispectral data. In this work, an extension model of *IHS-BT* approach (*eIHS-BT*) with a multi-optional framework to fuse optical/*SAR* data has been proposed and implemented into a Windows-based program. It has been demonstrated that the properties of the fusion results controlled by two adjustable parameters which allow user to balance the spatial and texture content of the fused image and chose one of image fusion methods, such as *IHS*, *BT*, *IHS-BT* and *SAR-Pan*. For multi-source image interpreting, the presented approach offers more options than the existed methods and a better understanding of the objects observed within the image scenes. One result of this work shows that using a suitable value for one parameter to fuse reasonable proportions of *SAR* and *Pan* information with *MS* imagery can give better performance for assisting and training *SAR* image interpreters than using a standard method to just fuse *SAR* with *MS* imagery. With the aids of the red-green viewer (RGV) and the geo-link function, the main source points of corner reflections will appear clearly and guide image interpreters to find targets which lead to the appearance of corner reflections. High resolution IKONOS and TerraSAR-X imagery are used to assess the proposed method. Overall assessment of the proposed method shows that it is a promising method and superior to the standard methods alone.

ACKNOWLEDGEMENTS

Authors would like to appreciate Richi Technology for TerraSAR-X imagery support. Richi Technology is also an agent for DigitalGlobe imagery in Taiwan. The authors also want to thank GeoEye for IKONOS imagery support.

REFERENCES

[1] Pohl C. and Genderen J. L., “Multisensor image fusion in remote sensing: Concepts, methods, and applications,” Int. J. Remote Sens., vol. 19, no. 5, pp. 823–854, 1998.

[2] Alparone L., Baronti S., Garzelli A., and Nencini F., “Landsat ETM and SAR image fusion based on generalized intensity modulation,” IEEE Trans. Geosci. Remote Sens., vol. 42, no. 12, pp. 2832–2839, Dec. 2004.

[3] Liu J., “Smoothing filter-based intensity modulation: A spectral preserve image fusion technique for improving spatial details,” Int. J. Remote Sens., vol. 21, no. 18, pp. 3461–3472, 2000.

[4] Chibani Y., “Additive integration of SAR features into multispectral SPOT images by means of the à trous wavelet decomposition,” ISPRS J. Photogramm. Remote Sens., vol. 60, pp. 306–314, 2006.

[5] Klonus S., and Ehlers M., “Pansharpening

with TerraSAR-X and optical data," TerraSAR-X Science Team Meeting, 2008.

[6] Liu L., and Ning N., "Multi-spectral and SAR Image Fusion Based on Wavelet and IHS Transform," Proc. of SPIE Vol. 7492, 74922D, 2009.

[7] Chen S., Zang R., Su H., Tian J. and Xia J., "SAR and Multispectral Image Fusion Using Generalized IHS Transform Based on àTrous Wavelet and EMD Decompositions," IEEE Sensors Journal, Vol. 10, No. 3, pp. 737-745, 2010.

[8] Oguz G. and Jie S., "An Optimal Fusion Approach for Optical and SAR Images," ISPRS Commission VII Mid-term Symposium "Remote Sensing: From Pixels to Processes", 2006.

[9] Tu, T. M., Lee, Y. C., Chang, C. P., and Huang, P. S., "Adjustable intensity – hue - saturation and Brovey transform fusion technique for IKONOS/QuickBird imagery," Optical Engineering, Vol. 44, No. 11, pp. 116-201, 2005.

[10] Ledley, R. S., Buas, M., and Golab, T. J., "Fundamentals of true-color image processing," IEEE Proceedings, 10th International Conference, Pattern Recognition Vol. 1, pp. 791-795, 1990.

[11] Tu T. M., Huang P. S., Hung C. L., and Chang C. P., "A fast intensity-hue-saturation fusion technique with spectral adjustment for IKONOS imagery," IEEE Geosci. Remote Sens. Lett., vol. 1, no. 4, pp. 309–312, Oct. 2004.

[12] Aiazzi B., Baronti S., and Selva M., "Improving component substitution pansharpening through multivariate regression of MS + Pan data," IEEE Trans. Geosci. Remote Sens., vol. 45, no. 10, pp. 3230–3239, Oct. 2007.

[13] Kalpoma K. A., and Kudoh J. I., "Image Fusion Processing for IKONOS 1-m Color Imagery," IEEE Transactions on GeoscienSensing, Vol. 45, No. 10, pp. 3075-3086, 2007.